Journal of Photochemistry and Photobiology A: Chemistry 212 (2010) 36–42

Contents lists available at ScienceDirect

Journal of Photochemistry and Photobiology A: Chemistry

journal homepage: www.elsevier.com/locate/jphotochem

Effect of metal cations on the fluorescence lifetimes of pyrene-labeled G-quadruplex probes

Anna Dembska, Bernard Juskowiak*

Faculty of Chemistry, A. Mickiewicz University, Grunwaldzka 6, 60-780 Poznan, Poland

ARTICLE INFO

Article history:
Received 26 January 2010
Received in revised form 8 March 2010
Accepted 24 March 2010
Available online 2 April 2010

Keywords:
Excimer
Fluorescence
G-quadruplex
Lifetime
Potassium probe
Pyrene

ABSTRACT

Fluorescence lifetime study of two probes abbreviated as Py-Htelom-Py and Py-TBA-Py, carrying pyrene moieties at both termini and sequences of human telomere and thrombin binding aptamer, respectively are reported. The effect of metal cations (sodium, potassium and strontium) on the photophysical processes was examined in order to elucidate factors that facilitate the production of excimer emission. The fluorescence spectra and emission kinetics data supported the conclusion that pyrene-quadruplex conjugate has multiple conformers in solution and that the relative orientation of pyrene and neighboring nucleobases (guanine, adenine, thymine) play a crucial role in determining both the rate of electron-transfer quenching of pyrene excited state and the efficiency of excimer emission.

1. Introduction

Guanine-rich sequences of DNA can form four-stranded structures called G-quadruplexes under specific cation conditions. Generally, three or four planar guanine quartets, stabilized by cyclic Hoogsteen hydrogen bonds, are stacked and held together by π–π attractive interactions. Interestingly, G-quadruplexes may have different topological structures depending on the oligonucleotide length and sequence as well as on environmental conditions [1]. Recently, we have reported fluorescent oligonucleotide probes based on the G-quadruplex scaffold for detection of K^+ ion [2–5]. Two strategies were exploited for the transduction of metal cation binding event, the fluorescence resonance energy transfer (FRET) [2,3] and excimer emission of the pyrene labels [4,5]. The second strategy is of particular interest since it enables an insight into label–label and label/nucleobases interaction processes. For example, the thrombin binding aptamer (TBA) with a $d(G_2T_2G_2TGTG_2T_2G_2)$ sequence gave efficient excimer emission in the presence of potassium [4] but the probe with the human telomeric sequence $d(G_3(T_2AG_3)_3)$ showed only quenching of the pyrene monomer emission without noticeable excimer contribution [5]. The origin of different spectral characteristics of both probes was attributed to the topological differences in their folded structures (quadruplexes) but the detail factors affecting performance of probes need further studies. On the other hand, steady-state based approaches of the fluorescence probes suffer from some limitations that could hamper their effectiveness in complex biological samples. For instance, they are difficult to apply directly to analyzing potassium in biological environments because of the interference of intense background signal caused by both light scattering and native protein fluorescence. The progress in solving these problems in bioanalysis can be achieved by applying the time-resolved fluorescence approach [6,7]. One special feature of the pyrene emission (monomer and excimer) is the very long fluorescence lifetime compared with other potential fluorescent species [8]. The lifetime of the pyrene excimer can approach 100 ns [8], whereas that for most of the biological background species is below 5 ns [9]. With time-resolved fluorescence measurements, potassium induced excimer signal can be separated from biological background interference. Direct monitoring of potassium level in complex biological samples might be carried out without any need of sample clean-up process.

Here, we report detailed steady-state and fluorescence lifetime studies on two fluorescent probes shown in Fig. 1, abbreviated as Py-Htelom-Py and Py-TBA-Py. They carry pyrene moieties at both termini and sequences of thrombin binding aptamer and modified human telomere (two terminal adenine nucleotides were inserted compared with previously reported probe [5]). The effect of metal cations (sodium, potassium and strontium) on the photophysical processes was examined in order to elucidate factors that may facilitate the production of excimer emission.

* Corresponding author. Tel.: +48 61 8291467; fax: +48 61 8658008.
E-mail address: juskowia@amu.edu.pl (B. Juskowiak).

1010-6030/$ – see front matter © 2010 Elsevier B.V. All rights reserved.
doi:10.1016/j.jphotochem.2010.03.009

2. Experimental

2.1. Pyrene-labeled oligonucleotides

Pyrene-labeled oligonucleotides (Fig. 1) were custom-synthesized by Sigma-Genosys Japan (Ishikari, Japan) and purified by reversed phase HPLC and their identities were confirmed by MALDI-TOF MS (Voyager™). Stock solutions of the oligonucleotides were prepared in Milli-Q water (Millipore, Billerica, MA). Other chemicals were of analytical grade. Sample solutions contained 1 μM oligonucleotide probe, 5 mM Tris–HCl buffer (pH 7.4) and required concentration of metal cation. Samples were heated at 90 °C for 5 min and then incubated overnight at 4 °C before measurements.

2.2. CD and fluorescence spectra

Circular dichroism (CD) spectra were recorded in the 230–450 nm spectral range with a Jasco J8100 Spectropolarimeter. Spectra were recorded at room temperature in a 1 cm path length quartz cell using 2 μM solution of a probe in 5 mM Tris–HCl buffer (pH 7.4) containing a selected metal cation at desired concentration. Steady-state fluorescence measurements were conducted with a Jasco FP6200 Fluorescence spectrophotometer using a 10 mm quartz cell; the spectra were not corrected. Samples were stirred and thermal equilibrated before recording of spectra. Fluorescence probes were excited at 344 nm and the emission spectra were recorded in the 300–600 nm spectral range. The cell compartment was thermostated at 25 °C and was equipped with a magnetic stirrer. Relative fluorescence quantum yields of probes (ϕ) were determined using pyrene butanoic acid (PBA) in Tris–HCl buffer as a reference compound using the standard relationship: $\phi = \phi_R(F(1-10^{-A_R}))/(F_R(1-10^{-A}))$ where A and F are absorbance and integrated fluorescence, respectively, the index R denotes reference solution. No attempt was made to deaerate the solutions since preliminary test showed negligible effect of such a sample treatment.

2.3. Fluorescence lifetime measurements

Fluorescence decays were obtained using a TCSPC (Time Correlated Single Photon Counting) method. Measurements were made with an IBH Consultants (Glasgow, Scotland) model 5000 fluorescence lifetime spectrometer equipped with the NanoLED type diode (λ_{exc} = 340 nm, fwhm = 800 ps) as an excitation source. The instrument is capable of measuring lifetimes as short as 400 ps. The standard procedure for performing these measurements included taking an instrument profile and counting photon signals until at least 5000 counts were collected at the maxima of the fluorescence decay histograms. Reconvolution of fluorescence decay curve was performed using the IBH Consultants Version 4 software. The quality of the fits was judged from the *chi square* values ($\chi^2 \leq 1.4$), a runs test, and the random distribution of weighted residuals. In TCSPC measurements, the fluorescence intensity was monitored at λ_{max} of emission band unless otherwise stated. Solvents were checked under the conditions used in the fluorescence decay measurements, and they were found to exhibit emission small enough to be negligible relative to their influence on the lifetimes measured.

Py-TBA-Py **Py - GGTTGGTGTGGTTGG - Py**

Py-Htelom-Py **Py - AGGGTTAGGGTTAGGGTTAGGGA - Py**

where Py = 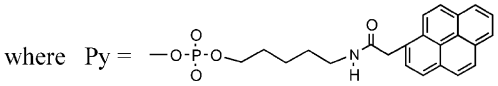

Fig. 1. The DNA sequences of pyrene-labeled G-quadruplex probes.

3. Results and discussion

3.1. CD spectra

Labeling with two pyrene tags may deteriorate folding properties of quadruplex-forming oligonucleotides. To ensure that tetraplex structures are formed by pyrene-modified oligonucleotides, the circular dichroism spectra were recorded for all investigated systems and results are shown in Fig. 2. Weak CD peaks are observed for both probes in Tris–HCl buffer alone, whereas addition of particular cations cause significant changes in CD spectra. Irrespective on the nature of metal cation added to the Py-TBA-Py solution, an appearance of positive bands near 295 and 245 nm and a negative band at 270 nm (Fig. 2A) is observed, which is consistent with the formation of the antiparallel quadruplex with a chair-type structure [10]. Low intensity of CD bands for sodium containing system reflects low quadruplex stabilizing effect of Na^+ ion [4,10]. Contrary to the TBA-based probe, the Py-Htelom-Py oligonucleotide showed CD spectra that differ significantly for particular metal cations (Fig. 2B), which reflect structural polymorphism of Htelom sequence. Spectrum for sodium quadruplex with two positive bands (295 and 245 nm) and a negative band at 270 nm resembles that for TBA probe and indicates formation of an antiparallel quadruplex, which was shown to possess a basket-type topology [11,12]. The presence of potassium induces the formation of a structure with the CD spectra having a strong positive band at 290 nm with a shoulder around 270 nm (Fig. 2B), characteristic of a hybrid-type parallel/antiparallel quadruplex that agrees with

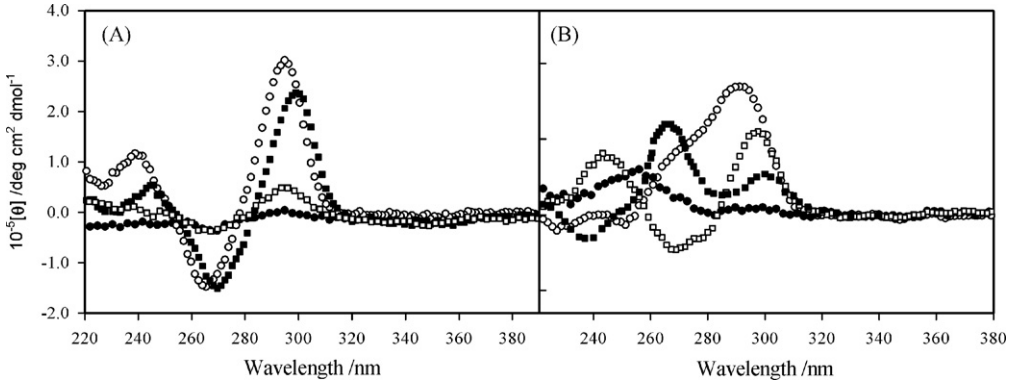

Fig. 2. Circular dichroism spectra of Py-TBA-Py probe (A) and Py-Htelom-Py probe (B) in the absence of metal cation (filled circles) and in the presence of: 100 mM KCl (open circles), 200 mM NaCl (open squares) and 200 mM $SrCl_2$ (filled squares). Probes were at concentration of 2 μM in Tris–HCl buffer pH 7.4.

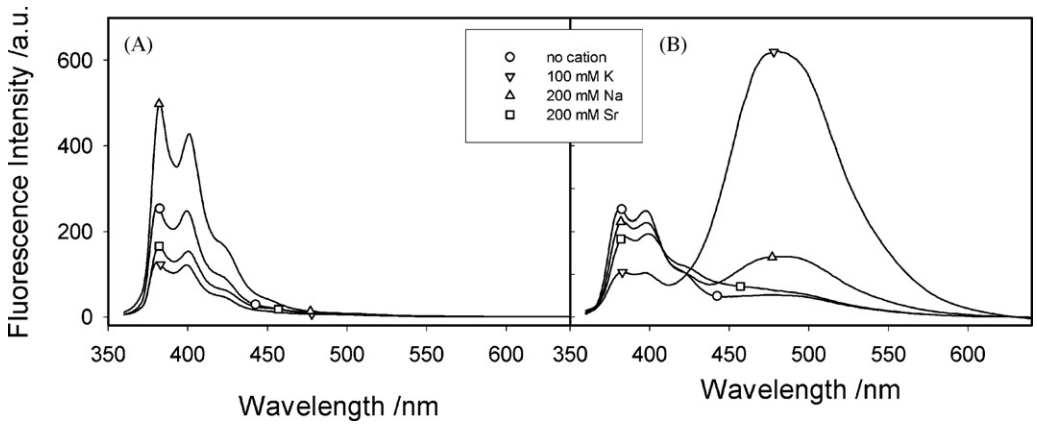

Fig. 3. Fluorescence spectra of pyrene-modified oligonucleotides in Tris–HCl buffer (pH 7.4): (A) Py-Htelom-Py and (B) Py-TBA-Py recorded in the absence of metal salt (circles) and the presence of 100 mM KCl (triangles down), 200 mM NaCl (triangles up) and 200 mM $SrCl_2$ (squares).

literature data [13,14]. Unlike K^+, addition of Sr^{2+} results in formation of a structure with a strong positive peak at 265 nm and a shoulder around 295 nm (Fig. 2B). This spectrum is indicative of formation of parallel-stranded intramolecular quadruplex with external or "propellel" loops [15,16]. Relatively strong intensity of a shoulder band at 295 nm may suggest an incomplete conversion of the antiparallel strontium quadruplex into parallel structure after thermal treatment [16] (a mixture of parallel and antiparallel-type quadruplexes is present in solution). Concluding, the CD spectra of metal/probe complexes are consistent with literature data for unmodified TBA and Htelom oligonucleotides [11–16], which means that conjugation of pyrene moieties has negligible effect on the folding properties of TBA and Htelom oligonucleotides. Also thermal stability of quadruplexes was not much affected by the attachment of pyrene tags. CD melting profiles (data not shown) indicated modest stabilizing effect of pyrene rings on the T_m values of probes (2–5 °C), in accordance with the previously reported results [5].

3.2. Steady-state fluorescence

Fig. 3 shows fluorescence emission spectra of oligonucleotide probes in the presence of selected metal cations (λ_{exc} = 340 nm) and the emission parameters are collected in Table 1. As expected, distinct differences in spectral characteristics are observed for Htelom and TBA probes. Only single emission band at *ca.* 390 nm with vibrational structure characteristic of the pyrene monomer fluorescence is observed for Htelom probe (Fig. 3A), which is consistent with results reported for shorter probe lacking adenine spacers [5]. On the contrary, TBA probe exhibits an additional long-wavelength emission band, especially in the presence of potassium ion (Fig. 3B) that is typical for the excimer emission. Interestingly, TBA systems show much lower fluorescence quantum yields comparing with Htelom-based systems (Table 1), for example, pyrene emission of the free Htelom probe is 3 times higher than that for free TBA probe. It should be noted however, that in both cases strong quenching operates since quantum yield of pyrene butanoic acid (not quenched by nucleobases) is several times higher (Table 1). It is generally accepted that anchoring the pyrene moiety to DNA oligonucleotide probe results in substantial decrease in fluorescence quantum yield, which is ascribed to the quenching processes due to the electron transfer (ET) between pyrene and DNA nucleobases (except for adenine [17]). Two mechanisms can be distinguished: (i) the quenching with the guanine as an electron donor and generation of a pyrene anion radical (ΔG for this ET reaction are reported between −0.03 and −0.33 V [17–22]) and (ii) the quenching with the participation of a pyrene cation radical and thymine and cytosine bases as electron acceptors (ΔG of *ca.* −0.5 V) are reported to be similar for thymine and cytosine [18]. One should consider also the GG and GGG consecutive tracks as very efficient electron donors in fluorescence quenching of pyrene with GGG being the most effective [22]. However, contribution from these electron donors into the overall quenching effect seems to be rather modest since fluorescence of TBA probe containing GG tracks is quenched more efficiently comparing with Htelom-based probe (Table 1), which disagrees with the order of reducing capability of guanine sites: G < GG < GGG [22]. Simple explanation for the more pronounced quenching for Py-TBA-Py may involve the relatively higher content of G and T bases in TBA oligonucleotide (exclusively G and T bases) whereas Htelom sequence contains also adenine (A) that is unable to quench pyrene fluorescence [17,19]. Concluding, the relative contribution of all mechanisms to the quenching depends on many factors including oligonucleotide sequence and its conformation, linker type and length, point of attachment of the fluorophore as well as relative orientation of the pyrene and nucleobase π-systems. [17,18,23–25].

Addition of metal cation (formation of quadruplex) affects seriously the emission of TBA probe (Fig. 3B). Even for free TBA probe, beside monomer fluorescence at 390 nm, one can see a broad emission at longer wavelength (480 nm). The effectiveness of particular salts in generation of excimer emission can be correlated with binding affinities of TBA to these cations since all of them form the same chair-type quadruplexes [1]. Comparing potassium and sodium TBA quadruplexes, only potassium is expected to form quadruplex quantitatively at concentration of 100 mM of metal cation as indicates from dissociation constant values (K_d = 7.33 and 272 mM for K^+ and Na^+, respectively [4]).

In case of the Py-Htelom-Py probe, there are no changes in the shape of emission when one compares spectrum of free probe with those for metal cation complexes (Fig. 3A). Addition of metal cation results only in the fluorescence intensity change, which extent depends on the nature and concentration of metal cation. The most pronounced quenching effect is caused by the interaction of potassium ion with Htelom probe; strontium ion also quenches pyrene fluorescence but to a lower extent. Only sodium quadruplex gives fluorescence enhancement (dequenching) effect. The enhancement of pyrene emission may be ascribed to the formation of a basket-type quadruplex, which probably requires disruption of a preorganization of the free oligonucleotide probe. Similar dequenching processes and subsequent fluorescence enhancement have been reported for NaCl effect on a TAMRA-labeled oligonucleotide [3] and for shorter Htelom probe [5]. The question arises whether the weak excimer emission contributes to the fluorescence spectra of the Htelom-based quadruplexes with

Table 1
Relative quantum yields (ϕ) and average lifetimes ($<\tau>$) for the quadruplexes of Py-Htelom-Py and Py-TBA-Py with metal cations.

Probe	Salt	Relative quantum yield, $\phi \pm 0.02$	Fraction of long-wavelength emission	Average lifetime[a], $<\tau>$ (ns)	
				390 nm	480 nm
PBA	No salt	1	0.06	85.4	–
Py-Htelom-Py	No salt	0.13	0.13	11.0	9.3
	100 mM KCl	0.05	0.16	6.3	3.4
	200 mM NaCl	0.24	0.12	18.4	8.3
	200 mM $SrCl_2$	0.07	0.16	5.4	4.3
Py-TBA-Py	No salt	0.04	0.34	6.2	4.3
	100 mM KCl	0.14	0.93	2.9	45.0
	200 mM NaCl	0.05	0.59	6.3	24.1
	200 mM $SrCl_2$	0.03	0.56	5.7	5.1

[a] Typical errors are of ±10–20%.

metal cations (Fig. 3A). To test such a possibility we calculated fractions of long-wavelength emission and the results are shown in Table 1. The fractions for Htelom probe systems approach values of 0.12–0.16 and are much lower compared to systems with TBA probe (0.37–0.93) but higher than that for pyrene butanoic acid (0.06). One should however exclude contribution from excimer emission since the fluoresce spectra of probes may be alternatively broadened by stacking interactions with nucleobases (e.g., guanine). Moreover, normalized spectra at the maximum of emission band of Htelom-based systems did not reveal any significant differences between free probe and its metal complexes.

3.3. Emission kinetics

Excitation wavelength in lifetime experiments was set at 340 nm (pyrene absorption band) and the excited state kinetics was monitored at 390 nm (pyrene monomer fluorescence) and at 480 nm characteristic of excimer emission. Preliminary reference experiments were carried out with buffer and unmodified oligonucleotides to assess the importance of background fluorescence. In both cases a weak emission was observed that originated from unknown impurities. Time-resolved emission from these samples was characterized by a lifetime shorter than 1 ns. This background emission was significantly lower than emission arising from the pyrene-labeled probes and was neglected in further study, but it may slightly contribute to the short lifetime emission signals. Examples of experimental decays for Py-TBA-Py (480 nm) and Py-Htelom-Py (390 nm) in the absence and the presence of metal cations are shown in Fig. 4.

Significant differences between decays for free and metal-bound probes are observed for both probes. Signal for Py-TBA-Py, monitored at the excimer emission ($\lambda = 480$ nm), decays slower after addition of metal ions (Fig. 4A). The most efficient lengthening of lifetime is observed for potassium/Py-TBA-Py quadruplex, in agreement with an appearance of excimer emission. Similar trend is observed for NaCl/Py-TBA-Py decay, but the effect is less pronounced. In case of $SrCl_2$, the observed changes in decay profile of Py-TBA-Py were rather small. It should be noted that decays of Py-TBA-Py probes monitored at 390 nm (monomer emission) exhibited profiles that indicated lifetime shortening (data not shown). Comparable metal cation effects were observed for Py-Htelom-Py probe irrespective of the monitoring wavelength (Fig. 4B). Similarity between decay traces recorded at 390 and 480 nm suggests that an additional long-wavelength emission is absent here, in good agreement with their steady-state spectra. Interestingly, while the average lifetimes undergo shortening for potassium and strontium quadruplexes, the formation of sodium quadruplex results in extension of the average lifetime (Table 1 and Fig. 4B).

The free pyrene label (1-pyrene butanoic acid, PBA) possesses high emission quantum yield ($\phi = 0.6$ [23]) and a single exponential decay with long lifetime, which is dependent on the media conditions. In not deaerated Tris–HCl buffer used in our experiments the lifetime for PBA is 85.4 ns (Table 1) that agrees with 83 ns obtained by Telser et al. in aerated phosphate buffer containing 100 mM NaCl [23]. On the other hand, Zahavy and Fox reported lifetime of 180 ns for PBA in deaerated phosphate buffer [19]. Attachment of the pyrene labels to the TBA or Htelom oligonucleotides leads to multiple emission decays. A tri-exponential equation $F(t) = A + B_1\exp(-t/\tau_1) + B_2\exp(-t/\tau_2) + B_3\exp(-t/\tau_3)$ was needed to fit the data both for free and metal-complexed probes. The relative amplitudes (fractions of the emitting species, α_i) were

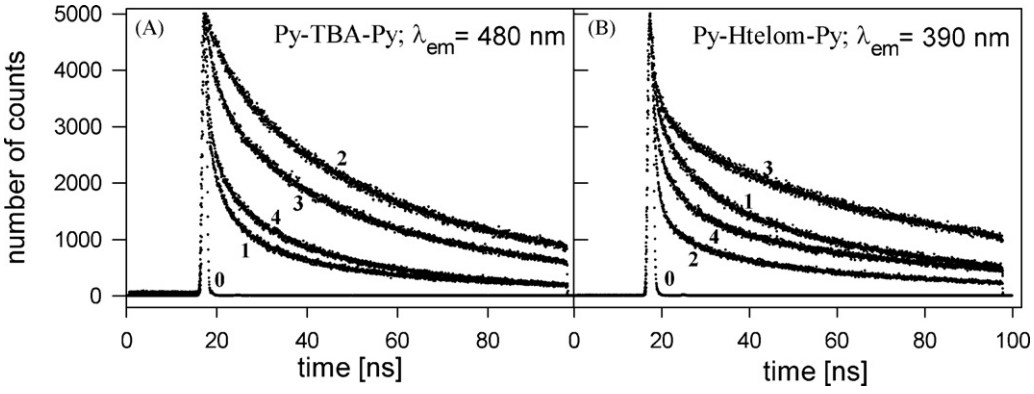

Fig. 4. Emission decay curves of Py-TBA-Py probe monitored at 480 nm (A) and Py-Htelom-Py probe monitored at 390 nm (B) in the absence of metal cation (1) and in the presence of: 100 mM KCl (2), 200 mM NaCl (3) and 200 mM $SrCl_2$ (4). Probes were at concentration of 1 μM in Tris–HCl buffer pH 7.4; the excitation was at 340 nm and trace 0 represents the lamp profile.

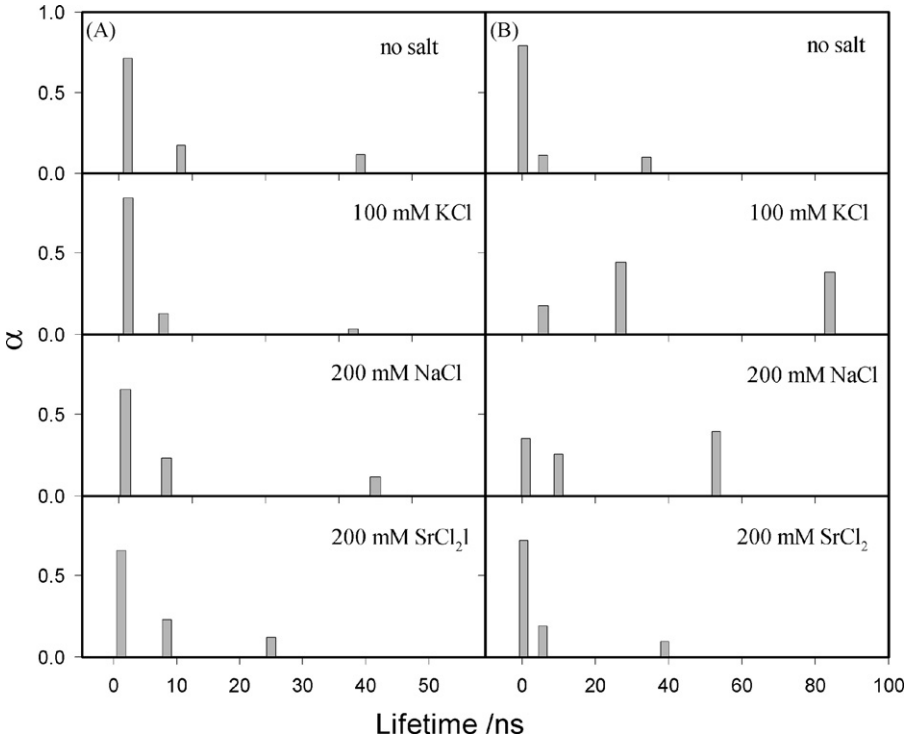

Fig. 5. Lifetime distribution diagrams for free Py-TBA-Py and its quadruplexes with metal cations, monitored at 390 nm (A) and 480 nm (B).

calculated using $\alpha_i = B_i / \sum_i B_i$ and average lifetimes <τ>, according to $< t >= \sum_i \alpha_i \tau_i$. Figs. 5 and 6 show diagrams of lifetime distribution for free probes and their metal cation quadruplexes. It should be noted that most decays are dominated by the short-lived component (for free probes above 70%) with lifetime about 1 ns or even below. Only in case of Py-TBA-Py/K^+ and Py-TBA-Py/Na^+ emission monitored at 480 nm, the fraction of short lifetime component is significantly lower (Fig. 5B). The medium lifetime components are in the range 6–8.5 ns (18–15%) for free probes and undergo small variations after addition of metal cations. Finally, the long-lived species have lifetimes of 33 ns (11%) and 60 ns (15%) for free TBA and

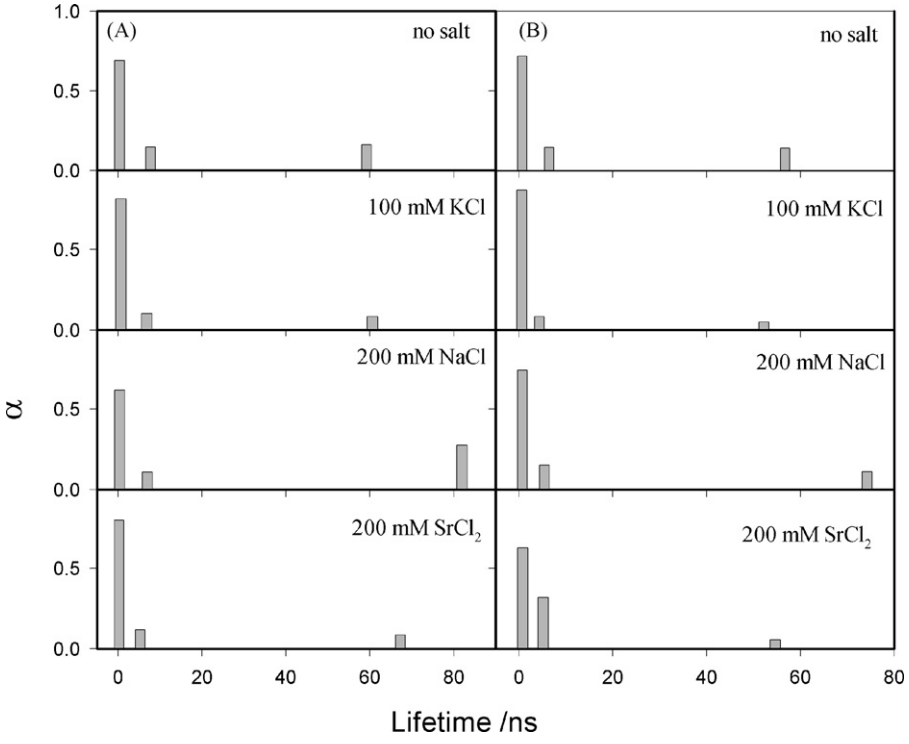

Fig. 6. Lifetime distribution diagrams for free Py-Htelom-Py and its quadruplexes with metal cations, monitored at 390 nm (A) and 480 nm (B).

Htelom probes, respectively. The much shorter lifetime for long-lived component of Py-TBA-Py is in good agreement with lower fluorescence quantum yield for TBA probe when compared with that for Py-Htelom-Py (Table 1).

Formation of quadruplexes in the presence of metal cations changes the lifetime distributions in all investigated systems. The most spectacular changes are observed for Py-TBA-Py/KCl and Py-TBA-Py/NaCl systems monitored at 480 nm (Fig. 5B) and for Py-Htelom-Py/NaCl system (Fig. 6). The long-lived component of ~30 ns (10%) for Py-TBA-Py probe was shifted to ~80 ns (KCl) and ~50 ns (NaCl) with a remarkable increase in population (~40%). The remaining two lifetimes (~1 and ~6 ns) were also shifted for KCl system to higher values of ~6 and 27 ns, respectively with remarkable fractional redistribution. Less pronounced changes for Na^+/TBA system are in good agreement with steady-state results already discussed. Lifetimes for K^+/Py-TBA-Py monomer emission monitored at 390 nm (Fig. 5A) exhibit changes that can be also explained by excimer formation. As result of pyrene–pyrene interactions the population of the long-lived component with lifetime of ~30 ns (11%) decreased significantly (3%) in the presence of potassium ion without particular shift in lifetime (Fig. 5A). Simultaneously, the relative fraction of the short-lived species with lifetime of ~1 ns (71%) increased markedly (85%).

The Htelom-based systems exhibited similar lifetime data for both monitoring wavelengths, in good agreement with the lack of excimer emission band in their fluorescence spectra. Results calculated for 390 nm seems to be more reliable due to the higher signal-to-noise ratio at this wavelength. Interestingly, free Py-Htelom-Py probe has the long-lived lifetime of ~60 ns, which is almost 2 times longer than that for TBA probe but still remarkable shorter than obtained for PBA. Addition of potassium has modest effect on the values of lifetimes but affected significantly their relative distribution. The population of the species with shortest lifetime increased from 69% to 82%, the fractions of medium and longest lifetime components decreased from 15% to 10% and from 16% to 8%, respectively (Fig. 6). Opposite effect was observed for sodium/Py-Htel-Py quadruplex, for which the lifetime of long-lived component and its fraction increased from ~60 ns (15%) to ~80 ns (28%) in the presence of 200 mM NaCl (Fig. 6A). Strontium ion also caused an increase in lifetime of long-lived component (67 ns) but because of a drop in population of this species (~8%) and a gain in fractions of short-lived species, the average lifetime decreased (Table 1). Efficient deactivation kinetics of the excited state of Py-Htelom-Py/potassium probe is in good agreement with strong fluorescence quenching observed in this system (Fig. 3), but the nature of the quenching seems to be static in origin since no lifetime shortening is observed.

As the three lifetimes characterize the emission decays of investigated systems, it is not necessarily true that there are only three distinct deactivation processes of pyrene excited state and that the particular lifetime τ_i denotes the same emitting component in different systems. There may be many such processes in the system and we do not intend to propose its microscopic description. The lifetime data presented here should be rather regarded as a qualitative measure of the pyrene–pyrene and pyrene–nucleobases interactions and will be discussed in relation to their quadruplex topologies. Therefore, one may conclude, that Py-TBA-Py/potassium quadruplex formation leads to the efficient label–label interactions that results in redistribution of the lifetimes of monomer excited state (shortening of the average lifetime) accompanied with the appearance of the excimer emission with much slower deactivation processes. Similar interaction model is valid for Na^+ and Sr^{2+}/TBA quadruplexes, but the effects are much smaller. The chair-type structure of the TBA quadruplex shown in Fig. 7A with the face-to-face arrangement of pyrene labels is undoubtedly responsible for the generation of excimer emission

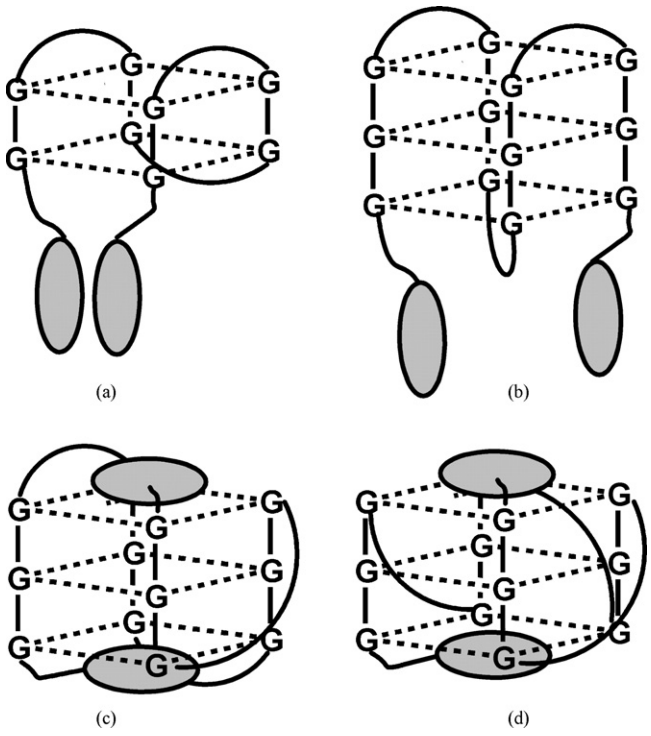

Fig. 7. Expected arrangement of pyrene labels (shadowed ovals) for different quadruplex structures: (A) a chair-type of Py-TBA-Py/M^{n+}, (B) a basket-type of Py-Htelom-Py/Na^+, (C) a hybrid-type of Py-Htelom-Py/K^+, and (D) a propeller-type of Py-Htelom-Py/Sr^{2+}.

[4,10]. The potassium ion with high binding affinity appeared to be the most effective, the Na^+/TBA quadruplex constant is considerably lower, thus quadruplexes are not developed quantitatively. Strontium ion stabilizes TBA quadruplex with comparable affinity to K^+ ion [10] whereas its efficiency in lifetime lengthening and generation of excimer emission is rather poor (Figs. 3B and 5B). Probably other factors may also play important role, for example, divalent metal cations stabilize quadruplexes in different way comparing with monovalent ones. They can stabilize a quadruplex both by coordination within the central channel of a quadruplex and by screening repulsion of backbone phosphate charges [1]. The ability of strontium ion to screen backbone repulsion is significantly higher than that of potassium or sodium ions, therefore Sr^{2+}/TBA quadruplex possesses more compact arrangement that may disturb in formation of excimer by pyrene labels. Small shift of band observed in CD spectra for K^+ and Sr^{2+}/Py-TBA-Py quadruplexes (Fig. 2A) are consistent with differences reported by Kankia and Marky for CD spectra of unmodified TBA quadruplexes, which were explained by the tightness of particular structures due to electrostatic interactions [10]. Even more spectacular differences between the chair-type structures of K^+ and Sr^{2+}/TBA quadruplexes revealed NMR studies [26,27]. As results of different binding stoichiometry (2:1 and 1:1 for K/TBA and Sr/TBA, respectively), two potassium ions are bound outside of the quadruplex core interacting additionally with thymines in the loops [26] while Sr^{2+} ion is localized in the center of the quadruplex [27].

Contrary to TBA, oligonucleotides with human telomere sequence are know to form quadruplexes that exhibit structural polymorphism in the presence of specific metal cations [11,13–16,28]. One can assume that nonfluorescent pyrene dimers and/or pyrene/nucleobase stacking complexes can be responsible for observed lifetime distribution. Formation of nonfluorescent pyrene dimers should be rather ruled out since they were not observed in similar TBA system. The quenching effect of potassium

and strontium ions should be discussed in terms of their quadruplex topologies. In both cases the formation of quadruplex proceeds probably without substantial rearrangement of preformed free probe structure (partially quenched). The final strong quenching should be linked to pyrene/nucleobase stacking interactions and/or dynamic quenching through electron transfer (ET) [5]. Two quadruplex structures, the hybrid- and the propeller-type (Fig. 7C and D, respectively) can explain observed efficient quenching in the presence of KCl and $SrCl_2$, respectively. It was shown recently that hybrid-type quadruplex dominates in KCl solution while Sr^{2+}/Htelom quadruplex was reported to adopt the parallel structure [13–16] and CD spectra recorded for our probes (Fig. 2B) agree with the literature data. Both these quadruplexes possess external guanine tetrads exposed to hydrophobic planar guest molecules. Pyrene moiety can thus effectively stack on the guanine tetrads facilitating static or ET quenching. Thymine bases present in lateral loops of hybrid-type quadruplex can quench additionally the emission of pyrene [17,20]. Sodium Htelom quadruplex possesses a basket-type structure [11], in which a diagonal TTA loop disturbs in both excimer formation and pyrene-guanine tetrad stacking as shown in Fig. 7B. As result, no excimer emission nor quenching effect were observed for this system. Instead, the dequenching effect is observed that supports the importance of the conformational factors for the pyrene quantum yield.

4. Conclusions

Results of the fluorescence steady-state and lifetime measurements of G-quadruplexes formed between metal cations (K^+, Na^+, Sr^{2+}) and the pyrene-modified oligonucleotides with sequences of thrombin binding aptamer (Py-TBA-Py) and human telomeric sequence (Py-Htelom-Py) were presented. All decays of investigated systems could be characterized by a tri-exponential rate. Calculated lifetimes and their fractional distribution depended on the sequence of attached oligonucleotide and the nature of metal cation that occupies tetraplex internal cavity. The monomer emission data reflected the extent of quenching of pyrene excited state upon interactions with nucleobases or with second pyrene molecule. The long-wavelength emission was ascribed to pyrene excimer formation that proved pyrene-pyrene interactions. On the other hand, structure of quadruplex affects seriously label–label and label–nucleobase interactions. The quadruplex topology that enables an efficient label–label interactions, thus generation of excimer emission with very long lifetime, appeared to be a chair-type structure formed by Py-TBA-Py probe. Next, the hybrid and propeller-type structures of Py-Htelom-Py quadruplexes facilitate deactivation of the excited state of pyrene due to stacking interactions between pyrene and guanine tetrads. Finally, Htelom quadruplex with a basket-type structure possesses a diagonal TTA loop, which disturbs in both pyrene–pyrene interactions and pyrene-guanine tetrad stacking.

The mechanism of fluorescence quenching of pyrene emission by attached oligonucleotide needs further studies involving nanosecond time-resolved laser flash photolysis and transient absorption measurements.

References

[1] S. Neidle, S. Balasubramanian (Eds.), Quadruplex Nucleic Acids, RSC Biomol. Sci., Cambridge, 2006.
[2] H. Ueyama, M. Takagi, S. Takenaka, A novel potassium sensing in aqueous media with a synthetic oligonucleotide derivative. Fluorescence resonance energy transfer associated with guanine quartet-potassium ion complex formation, J. Am. Chem. Soc. 124 (2002) 1428–14287.
[3] B. Juskowiak, E. Galezowska, A. Zawadzka, A. Gluszynska, S. Takenaka, Fluorescence anisotropy and FRET studies of G-quadruplex formation in presence of different cations, Spectrochim. Acta A 64 (2006) 835–843.
[4] S. Nagatoishi, T. Nojima, B. Juskowiak, S. Takenaka, A pyrene-labeled G-quadruplex oligonucleotide as a fluorescent probe for potassium ion detection in biological applications, Angew. Chem. Int. Ed. 44 (2005) 5067–5070.
[5] H. Hayashida, J. Paczesny, B. Juskowiak, S. Takenaka, Interactions of sodium and potassium ions with oligonucleotides carrying human telomeric sequence and pyrene moieties at both termini, Bioorg. Med. Chem. 16 (2008) 9871–9881.
[6] C.J. Yang, S. Jockusch, M. Vicens, N.J. Turro, W. Tan, Light switching excimer probes for rapid protein monitoring in complex biological fluids, Proc. Natl. Acad. Sci. U.S.A. 102 (2005) 17278–17283.
[7] J. Li, Z.C. Cao, Z. Tang, K. Wang, W. Tan, Molecular beacons for protein–DNA interaction studies, Methods Mol. Biol. 429 (2008) 209–224.
[8] F.M. Winnik, Photophysics of preassociated pyrenes in aqueous polymer solutions and in other organized media, Chem. Rev. 93 (1993) 587–614.
[9] V.L. Mosiman, B.K.P.L. Canterero, C.L. Goolsby, Reducing cellular autofluorescence in flow cytometry: an in situ method, Cytometry 30 (1997) 151–156.
[10] B.I. Kankia, L.A. Marky, Folding of the thrombin aptamer into a G-quadruplex with Sr^{2+}: stability, heat, and hydration, J. Am. Chem. Soc. 123 (2001) 10799–10804.
[11] Y. Wang, D.J. Patel, Solution structure of the human telomeric repeat d[$AG_3(T_2AG_3)_3$], Structure 1 (1993) 263–282.
[12] V. Dapic, V. Abdomerovic, R. Marrington, J. Peberdy, A. Rodger, J.O. Trent, P.J. Bates, Biophysical and biological properties of quadruplex oligodeoxyribonucleotides, Nucleic Acids Res. 31 (2003) 2097–2107.
[13] Y. Xu, Y. Noguchi, H. Sugiyama, The new models of the human telomere d[AGGG(TTAGGG)3] in K^+ solution, Bioorg. Med. Chem. 14 (2006) 5584–5591.
[14] A. Ambrus, D. Chen, J.X. Dai, T. Bialis, R.A. Jones, D.Z. Yang, Human telomeric sequence forms a hybrid-type intramolecular G-quadruplex structure with mixed parallel/antiparallel strands in potassium solution, Nucleic Acids Res. 34 (2006) 2723–2735.
[15] I.M. Pedroso, L.F. Duarte, G. Yanez, A.M. Baker, T.M. Fletcher, Induction of parallel human telomeric G-quadruplex structures by Sr^{2+}, Biochem. Biophys. Res. Commun. 358 (2007) 298–303.
[16] A. Wlodarczyk, P. Grzybowski, A. Patkowski, A. Dobek, Effect of ions on the polymorphism, effective charge, and stability of human telomeric DNA. Photon correlation spectroscopy and circular dichroism studies, J. Phys. Chem. B 109 (2005) 3594–3605.
[17] M. Manoharan, K.L.I. Tivel, M. Zhao, K. Nafisi, T.L. Netzel, Base-sequence dependence of emission lifetimes for DNA oligomers and duplexes covalently labeled with pyrene: relative electron-transfer quenching efficiencies of A, G, C, and T nucleosides toward pyrene, J. Phys. Chem. B 99 (1995) 17461–17472.
[18] T.L. Netzel, M. Zhao, K. Nafisi, J. Headrick, M.S. Sigman, B.E. Eaton, Photophysics of 2′-deoxyuridine (dU) nucleosides covalently substituted with either 1-pyrenyl or 1-pyrenoyl: observation of pyrene-to-nucleoside charge-transfer emission in 5-(1-pyreny1)-dU, J. Am. Chem. Soc. 117 (1995) 9119–9128.
[19] E. Zahavy, A.M. Fox, Photophysical quenching mediated by guanine groups in pyrenyl-N-alkylbutanoamide end-labeled oligonucleotides, J. Phys. Chem. B 103 (1999) 9321–9327.
[20] S. Fukuzumi, H. Miyao, K. Ohkubo, T. Suenobu, Electron-transfer oxidation properties of DNA bases and DNA oligomers, J. Phys. Chem. A 109 (2005) 3285–3294.
[21] C. Wanninger-Weiß, L. Valis, H.-A. Wagenknecht, Pyrene-modified guanosine as fluorescent probe for DNA modulated by charge transfer, Bioorg. Med. Chem. 16 (2008) 100–106.
[22] Y.A. Lee, A. Durandin, P.C. Dedon, N.E. Geacintov, V. Shafirovich, Oxidation of guanine in G, GG, and GGG sequence contexts by aromatic pyrenyl radical cations and carbonate radical anions: relationship between kinetics and distribution of alkali-labile lesions, J. Phys. Chem. B 112 (2008) 1834–1844.
[23] J. Telser, K.A. Cruickshank, L.E. Morrison, T.L. Netzel, C.K. Chan, DNA duplexes covalently labeled at two sites: synthesis and characterization by steady-state and time-resolved optical spectroscopies, J. Am. Chem. Soc. 111 (1989) 7226–7232.
[24] V. Shafirovich, S.H. Courtney, N. Ya, N.E. Geacintov, Proton-coupled photoinduced electron transfer, deuterium isotope effects, and fluorescence quenching in noncovalent benzo[a]pyrenetetraol-nucleoside complexes in aqueous solutions, J. Am. Chem. Soc. 117 (1995) 4920–4929.
[25] K. Kawai, H. Yoshida, A. Sugimoto, M. Fujitsuka, T. Majima, Kinetics of transient end-to-end contact of single-stranded DNAs, J. Am. Chem. Soc. 127 (2005) 13232–13237.
[26] V.M. Marathias, P.H. Bolton, Determination of DNA quadruplex structural type: sequence and potassium binding, Biochemistry 38 (1999) 4355–4364.
[27] X. Mao, L.A. Marky, W.H. Gmeiner, NMR structure of the thrombin-binding DNA aptamer stabilized by Sr^{2+}, J. Biomol. Struct. Dyn. 22 (2004) 25–33.
[28] G.N. Parkinson, M.H.P. Lee, S. Neidle, Crystal structure of parallel quadruplexes from human telomeric DNA, Nature 417 (2002) 876–880.